M&C 2017 - International Conference on Mathematics & Computational Methods Applied to Nuclear Science & Engineering, Jeju, Korea, April 16-20, 2017, on USB (2017)

A coupled neutronics and thermal-hydraulics modeling approach to the steady-state and dynamic behavior of MSRs

Tianliang Hu, Liangzhi Cao, Hongchun Wu, Kun Zhuang

School of Nuclear Science and Technology, Xi' an Jiaotong University, Xi' an, Shaanxi, 710049, China

Abstract - *A code system has been developed in this paper for the steady-state and dynamics simulations of MSRs. The homogenized cross section data library is generated using the continuous-energy Monte-Carlo code OpenMC which provides significant modeling flexibility compared against the traditional deterministic lattice transport codes. The few-group cross sections generated by OpenMC are provided to TANSY which is based on OpenFOAM to perform the steady-state full-core coupled simulations and dynamics simulation. For verification and application of the codes sequence, the simulation of a representative molten salt reactor core MOSART has been performed. For the further study of the characteristics of MSRs, steady-state results and several transients like the code-slug transient, unprotected loss of flow transient have been analyzed. The numerical results indicated that the TANSY code with the cross section library generated by OpenMC has the capability for the steady-state dynamics analysis and design of MSRs.*

I. INTRODUCTION

The Molten Salt Reactor (MSR) has been identified as one of the candidates for the generation- IV reactors. It presents a promising flexible option in response to the goals and criteria assigned to the future nuclear systems as its fuel-cycle sustainability, safety, environmental impact, proliferation resistance, diversity of applications and economics. Historically, MSRs have been the thermal-neutron reactors in which the neutrons in the reactor core are moderated by unclad graphite. Today both thermal and fast spectrum MSRs are being investigated. Since the fast spectrum MSRs has the unique advantages for the actinide burning and extending fuel resources except the common advantages owned by all MSRs like excellent neutron economy, flexibility of fuel cycle and inherent safety, we devote to the fast-spectrum MSRs in our research works. Moreover, the fast-spectrum MSRs have been selected as one of the GEN-IV reference reactors by the Generation IV International Forum [1][2].

The fluid nature of fuel in fast-spectrum MSRs gives extra flexibility in reactor design, fuel fabrication and recycling. But because of the applying of fluid fuel, MSRs have several special characteristics compared with the traditional solid-fuel reactors. First, the transport of the delayed neutron precursors by the fluid flow reduces the contribution of delayed neutrons to the chain reaction. As a consequence, the multiplication eigenvalue is not independent of the delayed neutron fraction and the fluid velocity field. The drawbacks related to the relative small value of the effective delayed neutron fraction in MSRs are the narrower margin to prompt-criticality and the lower capabilities for reactor control in case of prompt-criticality accident. Second, the fact that the fuel is dissolved in the coolant rather than separated from the coolant by the claddings and gas gap results in a much stronger coupling phenomenon between the neutronics and thermal-hydraulics. Third, the shape of the fuel is determined by the container because of the characteristics of fluid, the unstructured meshes are essential to model the complex geometry accurately. However most of the conventional reactor codes were developed for solid-fuel reactor and therefore not capable of taking liquid fuel flow into account. So in this study, we aim to develop a code system which can address all these modeling issues of MSRs.

In this paper, an OpenMC-TANSY codes sequence has been developed to analyze the steady-state and dynamics behavior of MSRs. The continuous-energy Monte-Carlo code OpenMC [3] is used to generate the homogenized cross-section data library which provides significant modeling flexibility compared against the traditional deterministic lattice transport codes. The few-group constants generated by OpenMC are provided to TANSY which is based on OpenFOAM [4][5] to perform the steady-state and dynamics simulations.

II. THEORIES AND METHODS

This work must be new and significant. Since the direct heterogeneous calculation for the whole core is quite complicated and time-assuming, the traditional "two-step" scheme for the neutron-physics calculations is adopted for the simulation of MSRs. The calculation procedure is described in Fig. 1. The simulation of MSRs core is done using the following three steps, i.e. the generation of the few-group cross section, the functionalization of the group constants and the full-core coupled neutronics and thermal-hydraulics simulation. Firstly, the few-group cross sections are generated by using openMC. Then the in-house developed code NECP-Lilac is used for the functionalization of the few-group constants. Finally, the full-core steady-state and dynamics analysis is performed by TANSY.

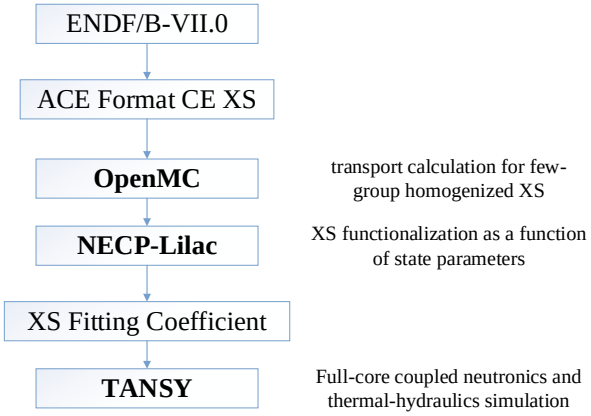

Fig. 1 "two-step" scheme

1. Neutronics modeling

The neutron-diffusion equation is applied for the neutronics simulation of the molten salt reactors in this paper. The formulation of the diffusion equation can be characterized as Eq. (1):

$$\begin{aligned}\frac{1}{v_g}\frac{\partial \phi_g(\vec{r},t)}{\partial t} &= \nabla D_g \nabla \phi_g(\vec{r},t) - \Sigma_{t,g}\phi_g(\vec{r},t) + \sum_{g'=1}^{G}\Sigma_{g'\to g}\phi_{g'}(\vec{r},t) \\ &+ \frac{1}{k_{eff}}(1-\beta_0)\chi_{p,g}\sum_{g'=1}^{G}(\upsilon\Sigma_f)_{g'}\phi_{g'}(\vec{r},t) \\ &+ \sum_{i=1}^{I}\chi_{d,i,g}\lambda_i C_i(\vec{r},t)\end{aligned} \quad (1)$$

$$\frac{\partial C_i(\vec{r},t)}{\partial t} + \nabla\cdot(\vec{U}C_i(\vec{r},t)) = \frac{\beta_i}{k_{eff}}\sum_{g'=1}^{G}(\upsilon\Sigma_f)_{g'}\phi_{g'}(\vec{r},t) - \lambda_i C_i(\vec{r},t)$$

The convection term in Eq. (1) represents the transport of delayed neutron precursors by the fluid flow, and the velocity field can be determined from the computational fluid dynamics simulation as discussed in the following section.

In this work, the multi-group neutron diffusion equations are discretized spatially using the unstructured-based finite volume method (FVM) which is quite widely used for the numerical simulation of a variety of applications involving fluid flow and heat and mass transfer. As for the time discretization, fully implicit scheme is applied for both neutron flux equations and delayed neutron precursor equations

2. Thermal-hydraulics modeling

The Computational Fluid Dynamic code OpenFOAM is employed to simulate the velocity and temperature distribution. The model of the fluid flow is based on the Reynolds-Averaged Navier-Stocks(RANS) equations. At current stage of MSRs calculation, the RANS model provides a good balance between the precision required for the thermal-hydraulics calculation and the computational effort. In our present work, the standard k-epsilon turbulence model have been adopted along with the standard wall functions. The basic principles of conservation of mass, momentum and energy can be characterized as shown inflowing:

$$\begin{aligned}&\frac{\partial \rho}{\partial t} + \nabla\cdot(\rho\vec{U}) = 0 \\ &\frac{\partial \rho\vec{U}}{\partial t} + \nabla\cdot(\rho\vec{U}\vec{U}) = -\nabla p + \nabla\cdot\vec{\tau} + \rho\vec{g} \\ &\frac{\partial \rho T}{\partial t} + \nabla\cdot(\rho\vec{U}T) = \nabla\cdot\frac{k}{C_p}\nabla T + S_T\end{aligned} \quad (2)$$

The thermal source consists primarily of the energy directly resulting from fission in reactors. The value of volumetric heat source can be determined and provided by the neutronics simulation as discussed in the previous section. The SIMPLE algorithm is employed for the steady-state problem and PISO algorithm for the transient problem.

3. Coupling scheme

In TANSY code, the neutron diffusion equations are solved both in fluid region (molten salt) and solid region (reflector). N-S equations and delayed neutron precursors balance equations are solved only in fluid region. Although the equations are solved in different regions, the overlapping part adopts the same spatial mesh. This allowed the adoption of a simple and computationally efficient cell-wise spatial coupling of the different variables, without requiring the implementation of mesh mapping techniques. The flowchart of the steady-state calculation and dynamics calculation are illustrated in Fig. 2 and 3.

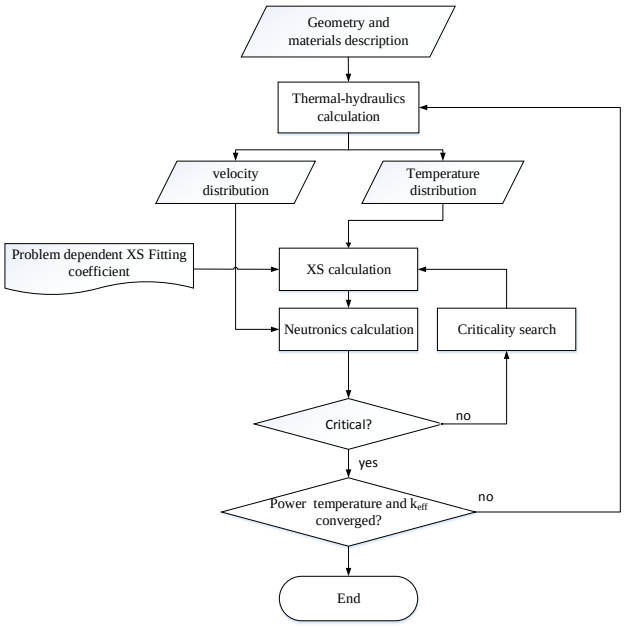

Fig. 2 flowchart of the steady-state calculation

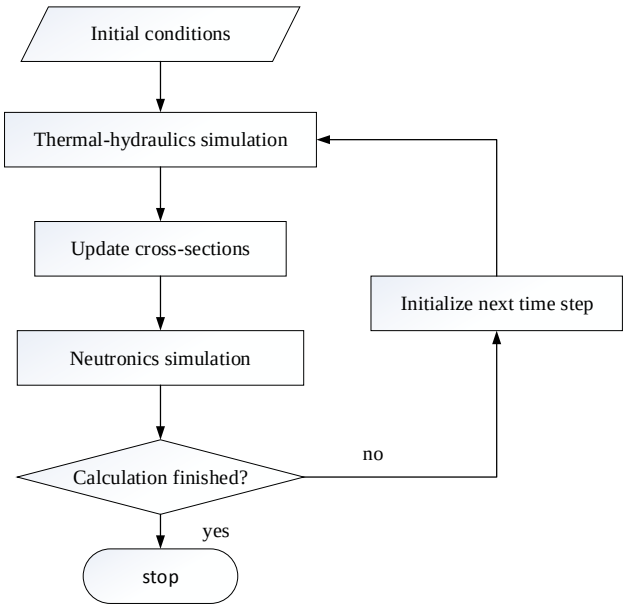

Fig. 3 flowchart of the dynamics simulation

According to the geometry and materials description, the thermal-hydraulics simulation is performed in the first place together with the node-wise power distribution obtained by the full-core neutronics simulation. After the convergence of the thermal-hydraulics simulation, the region-dependent macroscopic cross sections are updated using the temperature obtained by thermal-hydraulics simulation and the critical fuel concentration obtained by the criticality search. The mathematical expression can be written as:

$$\Sigma_x = f(\mathrm{T},\mathrm{fc}) = \sum_l \sum_n a_{l,n} T^l fc^n \qquad l = 0,3;\ n = 0,2 \tag{3}$$

Where T stands for the temperature of molten salt, fc stands for the fuel concentration.

In the following stage, the updated cross section and velocity field provided by computational fluid dynamics simulation are transferred to the full-core neutronics simulation module, then the neutron diffusion and delayed neutron precursors balance equations are solved. In the TANSY routine, the thermal-hydraulics and neutronics simulations are solved iteratively.

III. RESULTS

1. Verification of the neutronics solvers

The steady and transient-state neutronics solvers have been successfully programed based on the proposed model, benchmark calculation in reference are employed for verification. The total suite of tests conducted for the verification of the solvers ranges from two dimensional problems to there-dimensional problems from steady-state problems to transient-state problems. The test cases included herein are 2DIAEA [6], 3DIAEA [7], 2DLRA [8], 3DLRA [7] for the steady state calculation, and 3D-LMW for the transient state calculation.

The numerical results of the steady-state benchmark problems are summarize in Table 1. In table 1 ΔPmax and ΔPaverage are the maximum and average percentage errors of assembly power. The contours of the fast and thermal neutron flux distributions of 2D-IAEA are shown in Fig 4 and the normalized power distribution is given in Fig 4. It can be seen that the results show good agreement with the reference. The maximal difference exists in k_{eff} are all within 20 pcm and the maximal relative difference in the power distribution are all within 2%. Therefore, from the verification results, the development of the TANSY for solving the neutron-diffusion equation is correct.

Table I. Results of steady-state benchmark problems

Benchmark problems	K_{eff} error(10^{-5})	ΔP_{max} (%)	$\Delta P_{average}$ (%)
2DIAEA	1.5	0.318	0.103
2DLRA	4.7	1.13	0.374
3DIAEA	1.0	1.79	0.194
3DLRA	14.0	1.40	0.562

Reference				0.5849		
TANSY				0.5833		
Error				-0.27%		
			0.4706	0.6856	0.5972	
			0.4699	0.6862	0.5953	
			-0.15%	0.09%	-0.32%	
		1.1929	0.967	0.9064	0.8461	
		1.1936	0.9681	0.9068	0.8449	
		0.06%	0.11%	0.04%	-0.14%	
	1.4694	1.3451	1.1792	1.0705	0.9752	0.6921
	1.4695	1.3455	1.18	1.0711	0.9754	0.69
	0.01%	0.03%	0.07%	0.06%	0.02%	0.30%
1.4351	1.4799	1.3149	1.0697	1.0361	0.9504	0.7358
1.4349	1.4797	1.3153	1.071	1.0371	0.9507	0.7346
-0.01%	-0.01%	0.03%	0.12%	0.10%	0.03%	-0.16%
0.7456	1.3097	1.4537	1.2107	0.61	0.9351	0.9343	0.7549
0.7439	1.31	1.4535	1.2123	0.6092	0.9365	0.9347	0.7538
-0.23%	0.02%	-0.01%	0.13%	-0.13%	0.15%	0.04%	-0.15%

Fig. 4 Compassion of assembly power for 2DIAEA problem

The Langenbuch–Maurer–Werner (LMW) problem simulates an operational transient involving control rods (CRs) movement and is useful for the verification of space–time kinetics codes . The model is a simplified pressurized water reactor (PWR) core and is composed of two kinds of fuel assemblies. The number of neutron energy groups is two and the number of delayed precursors groups is six. Detailed macroscopic cross sections and kinetic parameters of each region can be found in the reference [9]. This problem simulates the motion of 2 groups of CRs, and the transient is initiated by withdrawing group 1 at 3.0 cm/s. CR group 1 is withdrawn to the top in 26.666 s, and group 2 is inserted to 120 cm during the time interval from 7.5 s to 47.5 s. The transient process lasts 60s.

The normalized power predictions during transient process by TANSY are given in Fig. 5. The results of TANSY are compared to the results of SPANDEX [10] with fine time step mesh. It can be seen that the results show good agreement with the reference, and the maximal relative difference is within 1.0%.

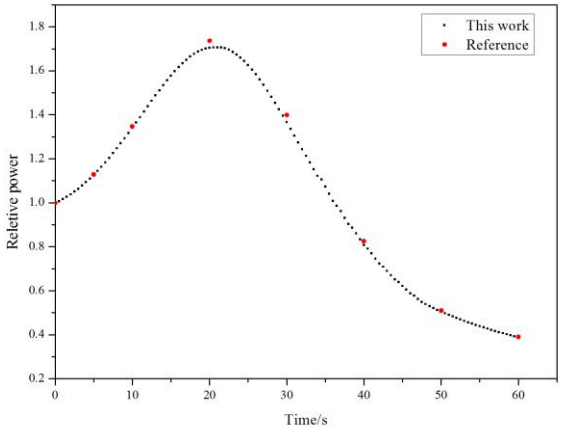

Fig. 5 The relative power for the 3D-LMW problem

2. Simulation of a simplified MSR design

In this work, a conceptual design of molten salt reactor called Molten Salt Actinide Recycler &Transmuter (MOSART) has been selected for the coupled neutronics and thermal-hydraulics simulation. The MOSART concept uses a single-fluid system fueled with the transuranic fluorides from LWR spent fuels. The design basic objective for MOSART [11][12] concept is to provide the fissile concentration and geometry of the fuel salt to obtain heat release of about 2400Mwt at conditions affording the effective transmutation of plutonium and minor actinides from LWR spent fuel without U-Th support. The concept design is displayed in Fig 6.

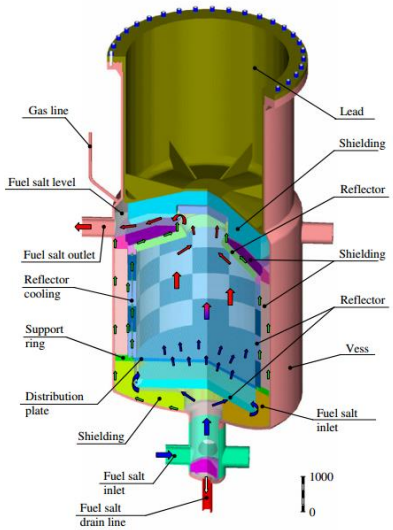

Fig. 6 MOSART concept core set-up

The 2400MWth MOSART system includes a cylindrical core having an intermediate to fast energy spectrum of neutrons. The concept design is displayed in Fig 6. No solid material is present in the core of this reactor as moderator. The inlet temperature of molten salt in core is 873K. The diameter and height of the cylindrical core are 3.4 m and 3.6 m, respectively. The core salt mass flow rate is 10000 kg/s. Average axial velocity of stream in core is 0.5m/s. The fuel salt enters the core through inlet radial window at the bottom of core and the salt flow is upward through the core to promote natural circulation. The fuel salt leaves the reactor vessel through outlet pipe attached to the top reflector. The out core circulation time is about 4 s.

The adopted MOSART core is a cylindrical blanket surrounded by a graphite reflector. In this preliminary studies a 2D R-Z core model was used in order to reduce the computational effort. The neutronics analysis was carried out using the 26-group cross-section data obtained by the openMC, and the radial reflector and axial reflector were all included to provide a more accurate power distribution. For the thermal-hydraulics calculation only the fluid region is considered, and the radial inlet window and distribution plate are ignored with a uniform velocity.

A. Steady-state analysis

The distribution of power and temperature at the rated operation state is dedicated in Fig. 7 and Fig. 8. It can be seen that the temperature increases along the axial direction and reaches the maximum at the core outlet. The maximum temperature of molten salt is about 1020k.

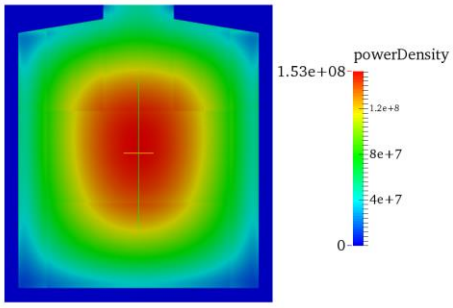

Fig. 7 Distribution of power density

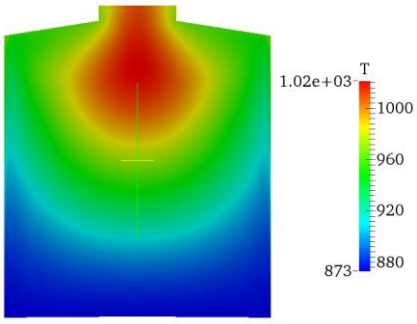

Fig. 8 Distribution of temperature

Six families of delayed neutron precursors are simulated in this study. The spatial dependency of the delayed neutron precursors are shown in Fig. 9. It can be seen that the peak concentration of delayed neutron precursors has a significant upward shift for family 1 to 5. It can also be concluded that the flow of molten salt has less effect on the delayed neutron precursors with shorter half-time.

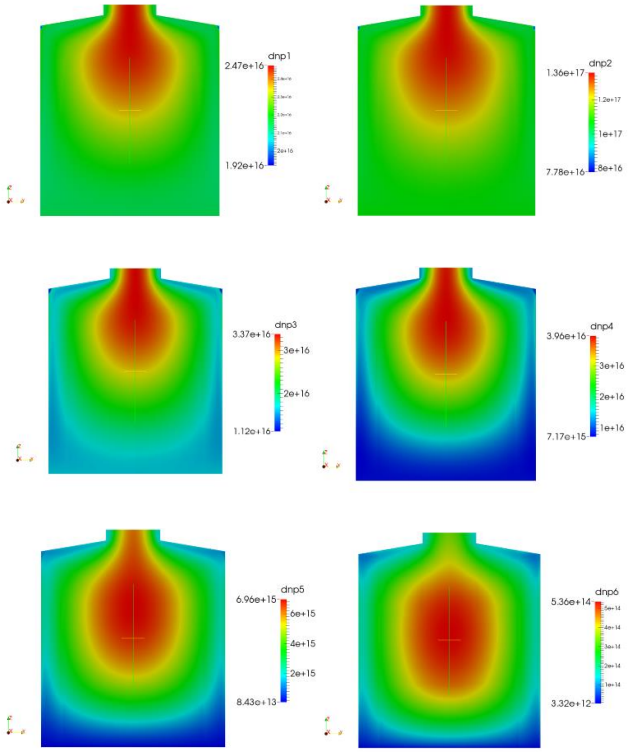

Fig. 9 Effect of fuel salt flow on the distribution of delayed neutron precursors

The spatial distributions of prompt neutron source and delayed neutron source are shown in Fig 10. It can be seen that the delayed neutron source and prompt neutron source have significant difference. In solid-fuel reactors, the delayed neutron source and prompt neutron source have the same distribution, but in MSRs due to the flow effect, the upward shift of delayed neutron precursors distribution results in the upward shift of delayed neutron source.

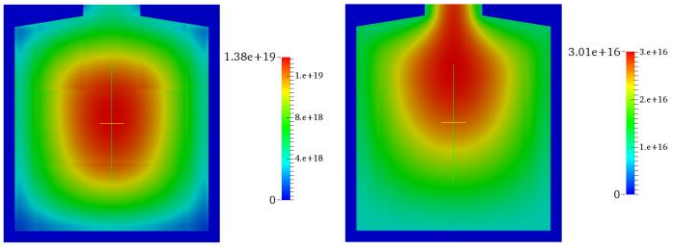

Fig. 10 Prompt neutron source and delayed neutron source

B. Dynamics analysis

The first transient simulated in this work is the code slug transient. The system response is studied in the case of code slug transient considering two situations: (a) 5m3 molten salt injected with temperature decrease of 75k; (b) 10m3 molten salt injected with temperature decrease of 75k. The calculated fission powers flowing the entry of code slugs into the core are shown in Fig. 11. Due to the strong negative feedback coefficient of molten salt, a decrease of inlet temperature cause a positive reactivity. As can be seen, the power increases sharply when the code slug flows into the core. But before the power has risen very high, the hot molten salt begins to enter the core behind the initial code slug and the consequent negative reactivity insertion because of the dopper and density effect finally reduces and stabilizes the power.

The average temperature and the outlet temperature is shown as a function of time in Fig. 12 and Fig. 13. The value of power and temperature during the transient are strongly coupled with each other. The power response to the system is mainly dependent upon the negative fuel temperature feedback. It can be seen from the result that the molten salt reactor is quite resistant to this kind of incident and tolerate high degree of cold slug quite well.

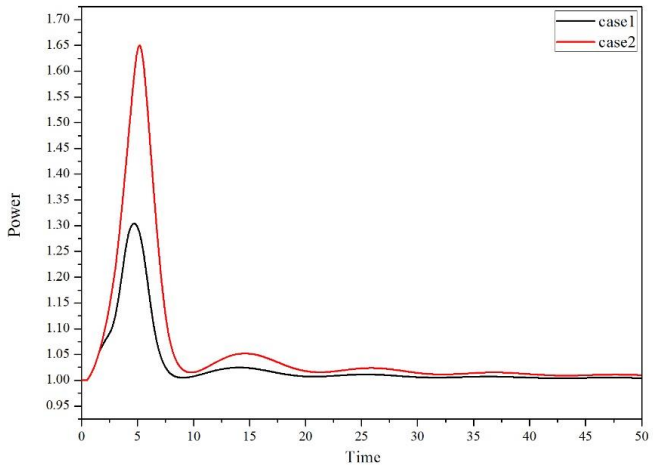

Fig. 11 Evolution of the power during the code-slug transient

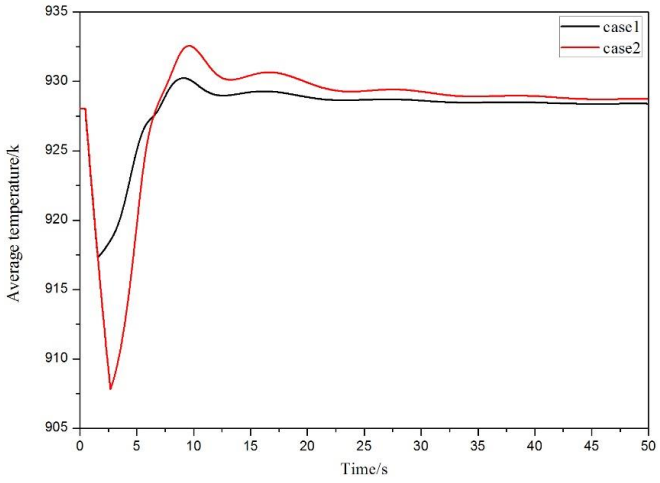

Fig. 12 Evolution of the average temperature during the code-slug transient

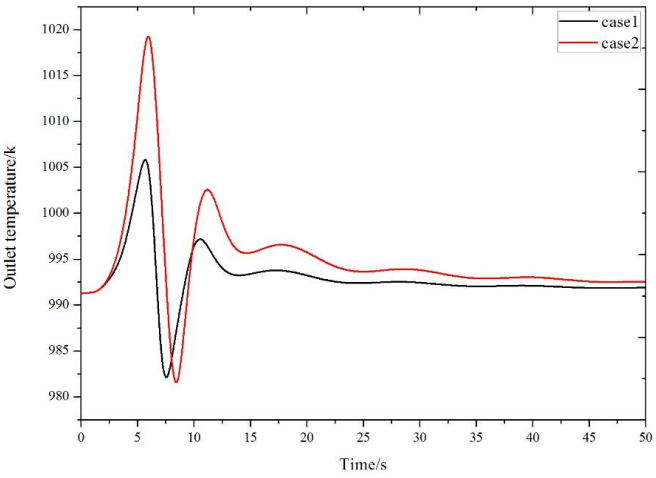

Fig. 13 Evolution of the outlet temperature during the code-slug transient

The second transient simulated in this work is the loss of flow transient. This transient could happen following the fuel circulation pump failure. The failure of the fuel pump is highly credible because it could result from the failure of the electrical power or from a mechanical defect. In order to represent this transient, it was simulated by reducing the fluid circulation rate according to the exponential law:

$$U_{in} = U_{in}(0)\,\mathrm{e}^{-\lambda_{pump}t} \tag{4}$$

The calculated fission power following the reduction of inlet velocity is displayed in Fig. 14. A reduction in heat removal from the core causes the average temperature rise, which affects the power response through its feedback reactivity coefficients. Fig. 14 denotes the power decrease at the transient beginning, and subsequently the stabilization at about the 65% of its initial value power. Fig. 15 denotes the evolution of the average temperature and outlet temperature during the loss of flow transient

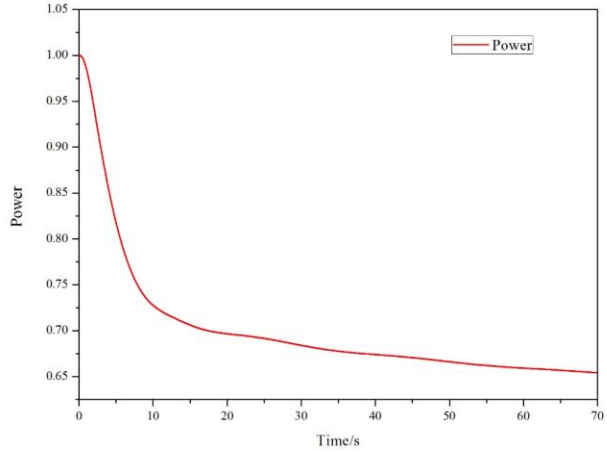

Fig. 14 Evolution of the power during the loss of flow transient

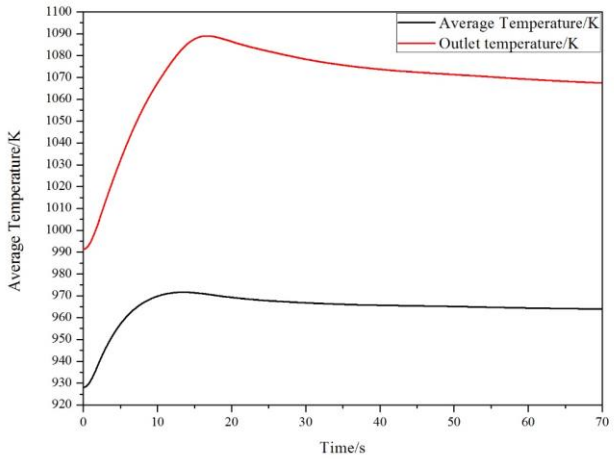

Fig. 15 Evolution of the average temperature and outlet temperature during the loss of flow transient

IV. CONCLUSIONS

In this study, the OpenMC-TANSY code sequence has been developed based on the "two-step" scheme for the steady-state and dynamics analysis of MSRs. The newly developed neutronics solvers in TANSY were verified by a series of benchmark problems including 2D-IAEA, 2D-LRA, 3D-IAEA, 3D-LRA and 3D-LMW, and in order to demonstrate the simulation capabilities of the OpenMC-TANSY codes sequence, the representative molten salt fast reactor MOSART has been simulated and analyzed in this paper. It can be concluded from this study that the developed code system takes into account the multiple levels of the coupling and resolves the interdependence between the different fields of MSRs.

ACKNOWLEDGMENTS

The authors wish to thank the National Natural Science Foundation of China (Grant No. 91226106) for financial support.

REFERENCES

1. Generation IV International Forum, 2002. A technology roadmap for Generation-IV nuclear energy systems, GIF-002-00. Issued by the US DOE Nuclear Energy Research Advisory Committee and the Generation IV International Forum.
2. FORSBERG, C.W., 2007. Thermal- and fast-spectrum molten salt reactors for actinide burning and fuel production. In: Proceeding of Global 2007, Boise, Idaho, USA.
3. ROMANO P K, FORGET B. The OpenMC Monte Carlo particle transport code[J]. Annals of Nuclear Energy, 2013, 51: 274-281.
4. WELLER H G, TABOR G, JASAK H, et al. A tonsorial approach to computational continuum mechanics using object-oriented techniques [J]. Computer in physics, 1998, 12(6):620-631
5. JASAK H, JEMCOV A, TUKOVIC Z. OpenFOAM: A C++ library for complex physics simulations[C]//International workshop on coupled methods in numerical dynamics. 2007, 1000:1-20.
6. E. Z. Muller, Z. J. Weiss, Benchmarking With the Multi-group Diffusion High-Order Response Matrix Method, Annals of Nuclear Energy, Vol.18, No.9, pp.535-544, 1991.
7. B. R. Bandini, A Three-dimensional Transient Neutronics Routine for the TRAC-PF1 Reactor Thermal Hydraulic Computer Code, Ph.D. thesis, Pennsylvania State University, May 1990.
8. R. D. Lawrence, A Nodal Green's Function Method for Multidimensional Neutron Diffusion Calculations, Thesis, University of Illionois, Urbana, 1979.
9. Ban Y, Endo T, Yamamoto A. A unified approach for numerical calculation of space-dependent kinetic equation[J]. Journal of nuclear science and technology, 2012, 49(5): 496-515
10. T.M. Sutton and B.N. Aviles, Diffusion theory methods for spatial kinetics calculation, Prog. Nucl. Energy 30(1996), pp. 119–182.
11. IGNATIEV, V., 2003. Neutronic properties and possible fuel cycle of a molten salt transmuter. In: Proceeding of the 2003 ANS/ENS International Winter Meeting (GLOBAL 2003), New Orleans, LA.
12. IGNATIEV, V., Feynberg, O., Gnidoi, I., Merzlyakov, A., Smirnov, V., Surenkov, A., Tretiakov, I., Zakirov, R., 2007. Progress in development of Li, Be, Na/F molten salt actinide recycler and transmuter concept. In: Proceedings of ICAPP, Nice, France, p. 75.